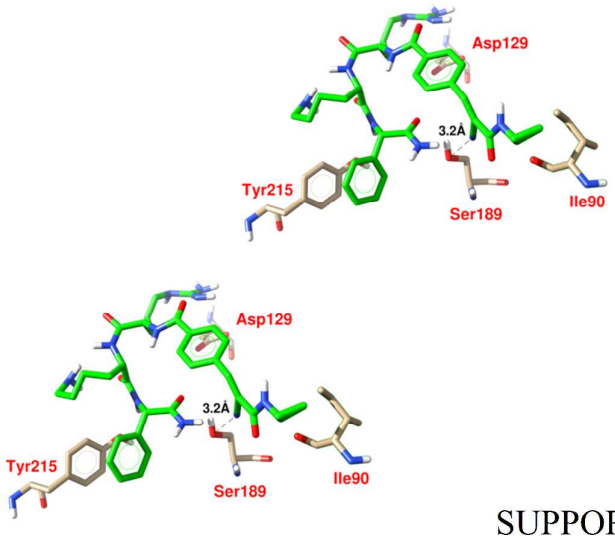

SUPPORTING INFORMATION

C-Terminal Residue Optimization and Fragment Merging: Discovery of a Potent Peptide-Hybrid Inhibitor of Dengue Protease

Mira A. M. Behnam, [†] Christoph Nitsche, [†] Sérgio M. Vechi, [†,‡] and Christian D. Klein*,[†]

[†]Medicinal Chemistry, Institute of Pharmacy and Molecular Biotechnology IPMB, Heidelberg University, Im Neuenheimer Feld 364, 69120 Heidelberg, Germany

[‡]Federal University of Alagoas (UFAL), Campus Arapiraca, NCEx, 57309-005 Arapiraca, Alagoas, Brazil

Contents

1. Chemical Reagents and Synthesis of Peptide Hybrids

All presented peptide and peptide-hybrid sequences were assembled by stepwise solid-phase synthesis using Fmoc-protected Rink amide resin, as previously described.[1-2] Unnatural amino acids were activated with HATU and DIPEA in DMF. The protected amino acids were purchased from Orpegen (Germany), Iris Biotech (Germany), Carbolution Chemicals (Germany), Bachem (Germany) and Sigma–Aldrich (Germany). HBTU was obtained Orpegen (Germany).HATU was purchased from Carbolution Chemicals (Germany). The Rink amide resin was purchased from Iris Biotech (Germany) and was of an average capacity of 0.65 mmol/g. All other chemicals or solvents were obtained from Sigma–Aldrich (Germany) and were of analytical grade.

2. HRMS and HPLC Data

The peptides and peptide-hybrids were obtained as solid powders after lyophilization and characterized by HR-ESI mass spectrometry on a Bruker microTOF-Q II instrument. Purity

was determined by HPLC on a Jasco HPLC system with a DAD detector on an RP18 column (ReproSil-Pur-ODS-3, Dr. Maisch GmbH, Germany, 5 µm, 50 mm × 2 mm). The conditions for the method used were: eluent A: water (0.1% TFA), eluent B: acetonitrile (0.1% TFA), injection volume: 10 µl, flow rate: 1 ml/min, gradient: 1% B (0.2 min), 100% B (7 min), 100% B (8 min), 1% B (8.1 min), 1% B (10 min). UV-detection was performed at 254 nm. All evaluated compounds were obtained with a purity of at least 95%, unless otherwise indicated.

No.	HRMS (ESI) for $[M+H]^+$			HPLC RT (min)	HPLC purity (254 nm)
	Molecular Formula	Calculated	Found		
2	$C_{22}H_{37}N_8O_5$	493.2881	493.2866	1.71	> 95%
3	$C_{28}H_{41}N_8O_4$	553.3245	555.3238	2.45	> 95%
4	$C_{22}H_{37}N_8O_4$	477.2932	477.2925	1.78	> 95%
5	$C_{21}H_{35}N_8O_4$	463.2776	463.2769	1.68	> 95%
6	$C_{24}H_{41}N_8O_4S$	537.2966	537.2957	2.17	> 95%
7	$C_{24}H_{41}N_8O_4$	503.3245	505.3243	2.15	> 95%
8	$C_{25}H_{43}N_8O_4$	519.3402	519.3398	2.24	> 95%
9	$C_{27}H_{39}N_8O_4$	539.3089	539.3079	2.25	> 95%
10	$C_{29}H_{41}N_8O_4$	565.3245	565.3248	2.45	> 95%
11	$C_{25}H_{43}N_8O_4$	519.3402	519.3388	2.27	> 95%
12	$C_{26}H_{37}N_8O_4$	525.2932	525.2932	2.26	> 95%
13	$C_{30}H_{42}N_9O_4$	592.3354	592.3345	2.56	> 95%
14	$C_{28}H_{41}N_8O_5$	569.3194	569.3193	2.21	> 95%
15	$C_{22}H_{37}N_8O_4$	477.2932	477.2925	1.76	> 95%

No.	HRMS (ESI) for $[M+H]^+$			HPLC RT (min)	HPLC purity (254 nm)
	Molecular Formula	Calculated	Found		
16	$C_{23}H_{39}N_8O_4$	491.3089	491.3083	1.90	> 95%
17	$C_{24}H_{39}N_8O_4$	503.3089	503.3078	1.99	> 95%
18	$C_{26}H_{37}N_8O_4$	525.2932	525.2928	2.14	> 95%
19	$C_{26}H_{37}N_8O_4$	525.2932	525.2924	2.07	> 95%
20	$C_{24}H_{37}N_8O_4$	501.2932	501.2916	1.95	> 95%
21	$C_{25}H_{41}N_8O_4$	517.3245	517.3234	2.12	> 95%
22	$C_{27}H_{40}N_9O_4$	554.3198	554.3198	1.79	> 95%
23	$C_{27}H_{40}N_9O_4$	554.3198	554.3196	1.83	> 95%
24	$C_{28}H_{40}N_9O_6$	598.3096	598.3091	2.60	92%
25	$C_{29}H_{40}N_9O_4$	578.3198	578.3192	2.48	> 95%
26	$C_{28}H_{47}N_8O_4$	559.3715	559.3712	2.84	> 95%
27	$C_{27}H_{45}N_8O_4$	545.3558	545.3561	2.54	> 95%
28	$C_{25}H_{43}N_8O_4$	519.3402	519.3399	2.36	> 95%
29	$C_{25}H_{43}N_8O_4$	519.3402	519.3396	2.29	> 95%
30	$C_{23}H_{39}N_8O_5$	507.3038	507.3032	1.79	> 95%
31	$C_{24}H_{41}N_8O_4$	505.3245	505.3243	2.10	> 95%
34	$C_{34}H_{45}N_{10}O_5$	673.3569	673.3553	1.96	> 95%
35	$C_{36}H_{48}N_9O_6S$	734.3443	734.3437	3.56	> 95%
36	$C_{36}H_{47}N_{10}O_5$	699.3725	699.3707	2.54	> 95%
37	$C_{38}H_{50}N_9O_6S$	760.3599	760.3593	3.53	95%
38	$C_{32}H_{49}N_{10}O_5$	653.3882	653.3871	2.72	> 95%
39	$C_{34}H_{52}N_9O_6S$	714.3756	714.3750	3.64	> 95%

3. NMR Data

^{1}H NMR spectra for selected compounds were recorded on Varian NMR instrument at 500 MHz, 300 K in D_2O. Chemical shifts (δ) are given in parts per million (ppm) in reference to the solvent HDO signal (4.79 ppm). Coupling constants (J) are given in Hertz (Hz). Multiplicity is reported as s (singlet), d (doublet), t (triplet), sept (septet), dd (doublet of doublet), tt (triplet of triplet) and m (multiplet), respectively.

9: ^{1}H NMR (500 MHz, D_2O): δ = 7.76 (dd, *J* = 8.4, 1.3 Hz, 2H), 7.68 – 7.63 (m, 1H), 7.55 (t, *J* = 7.7 Hz, 2H), 7.49 – 7.42 (m, 5H), 5.45 (s, 1H), 4.47 (dd, *J* = 8.1, 6.5 Hz, 4H), 3.36 (s, 2H), 3.15 (tt, *J* = 9.5, 4.8 Hz, 3H), 2.99 (t, *J* = 7.5 Hz, 3H), 2.00 – 1.38 (m, 15H).

13: ^{1}H NMR (500 MHz, D_2O): δ = 7.80 (d, *J* = 7.7 Hz, 2H), 7.71 – 7.63 (m, 2H), 7.56 (t, *J* = 7.7 Hz, 2H), 7.50 (d, *J* = 8.3 Hz, 1H), 7.28 – 7.22 (m, 2H), 7.16 (t, *J* = 7.5 Hz, 1H), 4.70 (dd, *J* = 8.5, 6.0 Hz, 2H), 4.39 (t, *J* = 7.3 Hz, 2H), 4.32 (dd, *J* = 8.5, 6.1 Hz, 2H), 3.38 (d, *J* = 6.0 Hz, 1H), 3.36 (d, *J* = 6.8 Hz, 1H), 3.25 (d, *J* = 8.5 Hz, 1H), 3.22 (d, *J* = 8.5 Hz, 1H), 3.16 – 3.06 (m, 3H), 2.93 – 2.80 (m, 3H), 1.87 – 1.45 (m, 11H), 1.40 – 1.18 (m, 4H).

25: ^{1}H NMR (500 MHz, D_2O): δ = 7.80 (d, *J* = 7.6 Hz, 2H), 7.72 (d, *J* = 8.1 Hz, 2H), 7.67 (t, *J* = 7.5 Hz, 1H), 7.57 (t, *J* = 7.7 Hz, 2H), 7.44 (d, *J* = 8.1 Hz, 2H), 4.70 (dd, *J* = 9.9, 5.3 Hz, 2H), 4.45 (t, *J* = 7.3 Hz, 2H), 4.31 (dd, *J* = 8.8, 6.0 Hz, 2H), 3.36 (s, 1H), 3.31 (dd, *J* = 14.0, 5.3 Hz, 1H), 3.24 (t, *J* = 7.0 Hz, 3H), 3.08 (dd, *J* = 14.0, 9.9 Hz, 1H), 2.94 (t, *J* = 7.7 Hz, 3H), 1.93 – 1.79 (m, 3H), 1.78 – 1.54 (m, 8H), 1.46 – 1.23 (m, 4H).

26: ^{1}H NMR (500 MHz, D_2O): δ = 7.84 – 7.79 (m, 2H), 7.70 – 7.64 (m, 1H), 7.56 (t, *J* = 7.7 Hz, 2H), 5.47 (s, 1H), 4.59 – 4.44 (m, 2H), 4.45 – 4.31 (m, 2H), 3.36 (d, *J* = 0.8 Hz, 2H), 3.26 (t, *J* = 6.9 Hz, 3H), 3.07 – 2.94 (m, 3H), 2.01 – 1.56 (m, 15H), 1.55 – 1.27 (m, 5H), 1.26 – 1.06 (m, 4H), 1.05 – 0.83 (m, 4H).

27: ^{1}H NMR (500 MHz, D_2O): δ = 7.80 (d, *J* = 8.3 Hz, 2H), 7.69 – 7.63 (m, 1H), 7.56 (t, *J* = 7.8 Hz, 2H), 4.59 – 4.47 (m, 2H), 4.43 (dd, *J* = 8.5, 6.2 Hz, 2H), 4.16 (d, *J* = 7.6 Hz, 1H), 3.43 – 3.30 (m, 2H), 3.26 (t, *J* = 7.1 Hz, 3H), 3.07 – 2.93 (m, 3H), 2.01 – 1.59 (m, 14H), 1.56 – 1.35 (m, 4H), 1.33 – 0.91 (m, 8H).

34: ^{1}H NMR (500 MHz, D_2O): δ = 8.26 (s, 1H), 8.05 – 8.00 (m, 2H), 7.90 (d, *J* = 8.5 Hz, 1H), 7.86 (d, *J* = 8.5 Hz, 1H), 7.51 – 7.41 (m, 5H), 5.48 – 5.43 (m, 1H), 4.56 – 4.51 (m, 1H), 4.50 – 4.45 (m, 2H), 4.42 (dd, *J* = 8.3, 6.1 Hz, 1H), 3.36 (s, 2H), 3.24 (t, *J* = 6.9 Hz, 1H), 3.20 – 3.10 (m, 2H), 3.06 – 2.96 (m, 2H), 2.92 (t, *J* = 7.7 Hz, 1H), 2.77 (sept, *J* = 3.7 Hz, 2H), 1.97 – 1.32 (m, 15H), 0.90 – 0.88 (m, 1H), 0.88 – 0.85 (m, 1H), 0.72 – 0.67 (m, 2H).

35: ^{1}H NMR (500 MHz, D_2O): δ = 7.93 – 7.86 (m, 2H), 7.84 (dd, *J* = 8.6, 2.2 Hz, 1H), 7.72 – 7.64 (m, 2H), 7.51 – 7.39 (m, 5H), 5.45 (d, *J* = 4.5 Hz, 1H), 4.55 – 4.50 (m, 1H), 4.50 – 4.45 (m, 2H), 4.42 (dd, *J* = 8.5, 6.3 Hz, 1H), 3.36 (s, 2H), 3.23 (t, *J* = 7.0 Hz, 1H), 3.20 – 3.10 (m, 2H), 3.03 – 2.98 (m, 1H), 2.97 – 2.86 (m, 2H), 2.10 – 1.15 (m, 24H).

38: ^{1}H NMR (500 MHz, D_2O): δ = 8.26 (s, 1H), 8.04 (d, *J* = 8.4 Hz, 2H), 7.91 (d, *J* = 8.3 Hz, 2H), 4.56 – 4.47 (m, 4H), 4.18 (s, 1H), 3.36 (s, 2H), 3.26 (t, *J* = 7.1 Hz, 3H), 3.02 – 2.96 (m, 3H), 2.77 (sept, *J* = 3.75 Hz, 2H), 2.01 – 1.67 (m, 12H), 1.56 – 1.37 (m, 3H), 1.02 (s, 9H), 0.88 (dd, *J* = 7.3, 1.8 Hz, 2H), 0.72 – 0.67 (m, 2H).

39: ^{1}H NMR (500 MHz, D_2O): δ = 7.94 – 7.90 (m, 2H), 7.89 (s, 1H), 7.71 (d, *J* = 8.3 Hz, 2H), 4.61 – 4.42 (m, 4H), 4.19 (s, 1H), 3.36 (s, 2H), 3.26 (t, *J* = 6.8 Hz, 3H), 2.99 (t, *J* = 7.6 Hz, 3H), 2.21 – 1.56 (m, 20H), 1.56 – 1.33 (m, 4H), 1.02 (s, 9H).

4. Determination of Reactivity towards Glutathione

GSH-reactivity was evaluated for compounds incorporating electrophilic N-terminal caps (**I** and **II**). For this purpose, 10 µl of the compound stock solution (10 mM in DMSO) and 10 µl GSH stock solution (10 mM in H_2O) were dissolved in Tris buffer (50 mM Tris–HCl, pH 9),

resulting in a final concentration of 100 µM of the test compound and GSH. Aliquots (100 µl) of the reaction mixture were taken at time intervals (every 30 minutes over a period of 3 hours) and the reaction was stopped by quenching with 10 µl phosphoric acid solution (10% in H_2O). The quenched samples were analyzed by HPLC using the method described above (purity assessment). The amount of the unreacted N-capped peptide was monitored and the concentration at each time-point was calculated by comparing the peak area with the initial signal (t =0, c = 100 µM). For the peptides incorporating the *N*-cyclopropyl cyanoacrylamide cap (**I**), **32**, **34**, **36**, **38**, the concentration decrease after 1 hour was below 25 % (range: 22–25 %). For the peptides incorporating the *N*-cyclopentyl thiazolidinedione cap (**II**), **33**, **35**, **37**, **39**, the concentration decrease after 1 hour was below 8% (range: 4–8 %). The experiment was repeated for all test compounds, using the same procedure but without addition of GSH, to evaluate the stability of the compounds in Tris buffer. For samples quenched after 1 hour, with and without GSH, LC-MS analysis was carried out using an Agilent HPLC system with MWD detector combined with the Bruker microTOF-Q II instrument on a RP-18 column (ReproSil-Pur-ODS-3, Dr. Maisch GmbH, Germany, 5 µm, 50 mm × 2 mm). The conditions for the method used were: eluent A: water (0.1% HCO_2H), eluent B: acetonitrile (0.1% HCO_2H), injection volume: 10 µl, flow rate: 0.4 ml/min, gradient: 5% B (1 min), 95% B (10 min), 5% B (10.1 min), 5% B (12 min). UV-detection was performed at 214 nm, 254 nm and 280 nm. Chromatograms recorded at 254 nm were used for calculations. GSH could be detected with the method used and showed minimal decrease in concentration (less than 4%) in all tested samples containing GSH, in comparison to a blank of just GSH and Tris buffer, prepared in the same concentration (10 µl of 10mM GSH stock solution and 990 µl Tris buffer) without any test compound. For the peptides incorporating the *N*-cyclopentyl thiazolidinedione cap (**II**), **33**, **35**, **37**, **39**, GSH-adduct formation did not exceed 4% after 1 hour, and 1-3% degradation products of the compounds in the buffer were found. For the peptides incorporating the *N*-cyclopropyl cyanoacrylamide cap (**I**), **32**, **34**, **36**, **38**, again GSH-

adduct formation did not exceed 4%. 18-20% of the N-cyclopropyl cyanoacrylamides underwent degradation in the buffer. The degradation product was analyzed by HR-ESI, and is expected to be the aldehyde with the general formula (CHO-Bz-Arg-Lys-X-NH_2, where X is the C-terminal amino acid), which is generated from a reverse Knoevenagel reaction. Cyanoacrylates are reported in literature to undergo hydrolysis in aqueous basic medium by a reverse Knoevenagel reaction to generate aldehyde degradation products.[3-4]

5. Sequence Alignment and Homology Modeling

The crystal structure of NS2B/NS3 from DEN serotype 3 in complex with a ligand (PDB ID: 3U1I, resolution 2.3 Å) was used as a template to build a dengue serotype 2 homology model.[5] The homology model of Den2V was constructed using the residues 50-88 (NS2B) and -1-10; 16-171 (NS3) from the template structure 3U1I. The alignment between template (3U1I) and target sequence (primary structure of the DEN NS2B-NS3 protease construct used in our laboratory) was calculated using Clustal Omega (**Figure S1**).[6] According to the alignment, the overall sequence identity between the DEN NS2B-NS3 protease construct used in our laboratory and 3U1I is 69%. Homology modelling was done using MODELLER 9v11 with python script commands and default parameters.[7] From the 100 models generated we chose that with the smallest values of DOPE and GA341. The selected model was then evaluated using PROFIT,[8] PROCHECK[9] and CHIRON.[10]

6. Quality of the Homology Model

The geometrical quality of the created homology model was evaluated using the program PROCHECK. The results revealed that 90% of the residues of the model are located in the most favored regions, 10% are located in the "generously allowed" regions and there was no residue of the model in the disallowed regions. We also compare the structures of the homology model and the experimental structure 3U1I using the least-squares fitting approach implemented in the program PROFIT which indicated a RMSD of 0.195 Å. The clashes in the

protein evaluated by the program CHIRON exhibited a clash score smaller than the acceptable value of 0.02 kcal mol^{-1} $contact^{-1}$. These results confirm that the predicted protein homology model has sufficient stereochemical quality, has a high structural similarity and does not present any severe steric clashes that could lead to artifacts of model building.

7. Docking Procedure

Autodock Vina 1.1.2 (AD Vina) was used to perform the docking studies and investigate the binding mode between selected compounds and the binding site of the homology model. Autodock Vina utilizes the Iterated Local Seach global optimizer algorithm which performs sequential steps consisting of a mutation and a local optimization, with each step being accepted according to the Metropolis criterion.[11] All the calculations were performed on an Intel(R) Core(TM)2 Quad CPU Q9450 @ 2.66 GHz running open SuSE 11.0. The structure of the ligands was optimized using the MM2 method and saved as a mol2 file. AD Vina was used with docking parameters at default values. Polar hydrogen atoms were added to the homology model, non-polar hydrogen atoms were merged and Kollman charges were assigned by default. For the ligands, non-polar hydrogen atoms were merged and Gasteiger charges assigned. All these docking preparation were performed with Autodock Tools.[12] The grid spacing was 1.0 and the size of the docking grid was 23 Å, 29 Å and 26 Å. Molecular graphics and analyses were also performed with the UCSF Chimera package v.1.9.[13]

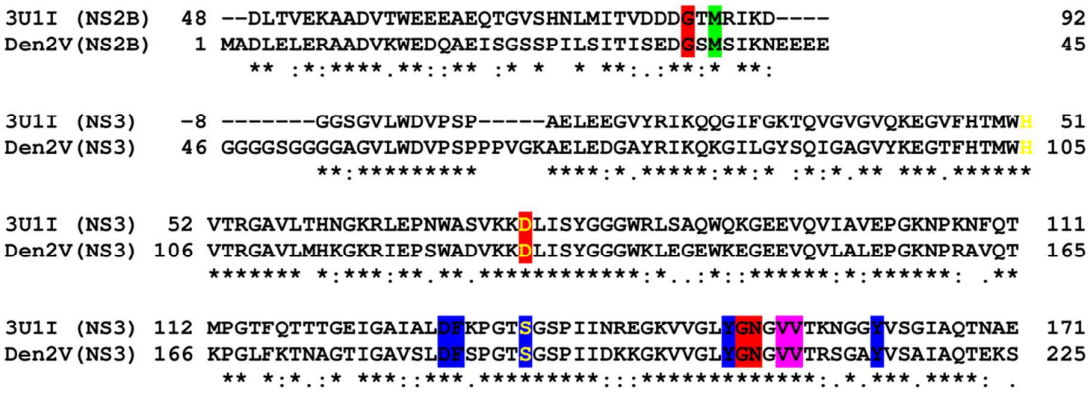

Figure S1. Sequence alignment of protein 3U1I and the DEN 2 NS2B-NS3 expression construct used in our laboratory. The numbers on the left and right refer to the amino acid positions. Identical residues are represented by asterisks and similar residues by colons and dots. The catalytic triad is shown in yellow whereas important residues located in the S_1, S_2, S_3 and S_4 pockets are shown in blue, red, green and pink, respectively.

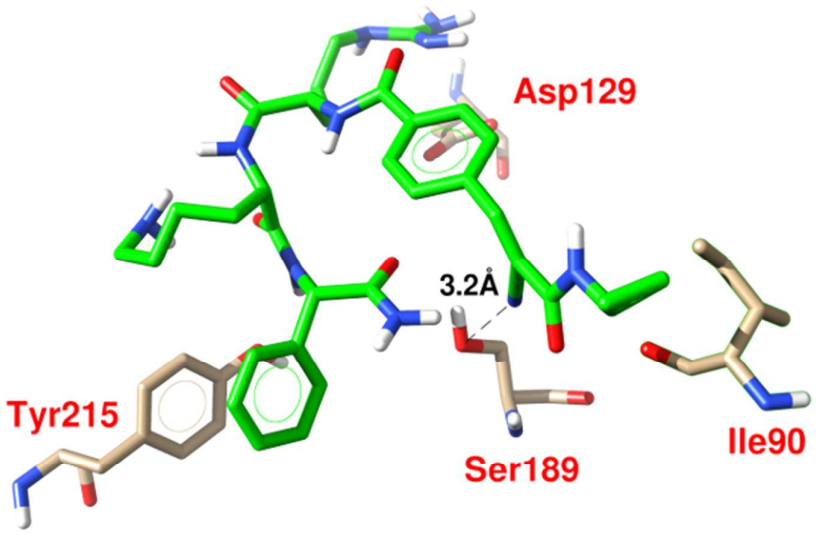

Figure S2. Docking pose of a cyanoacrylamide congener (cpd. 34) to the DEN-2 homology model. The nitrile group nitrogen is 3.2 Angstroms distant from the serine oxygen. A proton transfer from serine to the nitrile could trigger the formation of an imidate adduct between the inhibitor and the active-site serine.

Table S1. Total number of amino acid residues involved in hydrogen bonding and non-bonded interactions with the ligand within 3.9 Å calculated using the program HBPLUS, as implemented in LigPlot+.[9, 14] In yellow are represented the common residues between the pose generated by AD Vina and the covalent bound ligand of 3U1I.

	Cap-Arg-Lys-Phg-NH_2 (AD Vina)	**Bz-Nle-Lys-Arg-Arg-H (3U1I)**
Intermolecular hydrogen bonding interactions	Gly207B	Tyr161B (Tyr215B)
	Gly205B	Gly153B (Gly207B)
	Ser189B	Asn152B (Asn206B)
		Gly151B (Gly205B)
		Ser135B (Ser189B)
		Phe130B (Phe184B)
		Asp129B (Asp183B)
		His51B (His105B)
		Mer84A (Met37A)
Non-bonded interactions	Tyr215B	Tyr161B (Tyr215B)
	Arg211B	Val155B (Val209B)
	Val209B	Gly153B (Gly207B)
	Val208B	Asn152B (Asn206B)
	Gly207B	Gly151B Gly205B)
	Asn206B	Tyr150B (Tyr204B)
	Gly205B	Ser135B (Ser189B)
	Tyr204B	Phe130B (Phe184B)
	Ser189B	Asp129B (Asp183B)
	Phe184B	His51B (His105B)
	Asp183B	Arg85A (Ser38A)*
	Asp129B	Met84A (Met37A)
	His105B	
	Glu43A	
	Asn41A	
	Ile39A	
	Met37A	
	Ser36A	

8. References

1. Nitsche, C.; Behnam, M. A. M.; Steuer, C.; Klein, C. D., Retro peptide-hybrids as selective inhibitors of the Dengue virus NS2B-NS3 protease. *Antiviral Res.* **2012,** *94* (1), 72-79.

2. Nitsche, C.; Schreier, V. N.; Behnam, M. A. M.; Kumar, A.; Bartenschlager, R.; Klein, C. D., Thiazolidinone–Peptide Hybrids as Dengue Virus Protease Inhibitors with Antiviral Activity in Cell Culture. *J. Med. Chem.* **2013,** *56* (21), 8389-8403.

3. Leonard, F.; Kulkarni, R. K.; Brandes, G.; Nelson, J.; Cameron, J. J., Synthesis and degradation of poly (alkyl α-cyanoacrylates). *J. Appl. Polym. Sci.* **1966,** *10* (2), 259-272.

4. Bootz, A.; Russ, T.; Gores, F.; Karas, M.; Kreuter, J., Molecular weights of poly(butyl cyanoacrylate) nanoparticles determined by mass spectrometry and size exclusion chromatography. *Eur. J. Pharm. Biopharm.* **2005,** *60* (3), 391-399.

5. Noble, C. G.; Seh, C. C.; Chao, A. T.; Shi, P. Y., Ligand-Bound Structures of the Dengue Virus Protease Reveal the Active Conformation. *J. Virol.* **2012,** *86* (1), 438-446.

6. Sievers, F.; Wilm, A.; Dineen, D.; Gibson, T. J.; Karplus, K.; Li, W.; Lopez, R.; McWilliam, H.; Remmert, M.; Söding, J.; Thompson, J. D.; Higgins, D. G., Fast, scalable generation of high-quality protein multiple sequence alignments using Clustal Omega. *Mol. Syst. Biol.* **2011,** *7* (1).

7. Šali, A.; Blundell, T. L., Comparative Protein Modelling by Satisfaction of Spatial Restraints. *J. Mol. Biol.* **1993,** *234* (3), 779-815.

8. McLachlan, A., Rapid comparison of protein structures. *Acta Crystallogr. Sect. A: Found. Crystallogr.* **1982,** *38* (6), 871-873.

9. Laskowski, R. A.; Swindells, M. B., LigPlot+: Multiple Ligand–Protein Interaction Diagrams for Drug Discovery. *J. Chem. Inf. Model.* **2011,** *51* (10), 2778-2786.

10. Ramachandran, S.; Kota, P.; Ding, F.; Dokholyan, N. V., Automated minimization of steric clashes in protein structures. *Proteins: Struct. Funct. Bioinform.* **2011,** *79* (1), 261-270.

11. Trott, O.; Olson, A. J., AutoDock Vina: Improving the speed and accuracy of docking with a new scoring function, efficient optimization, and multithreading. *J. Comput. Chem.* **2010,** *31* (2), 455-461.

12. Morris, G. M.; Huey, R.; Lindstrom, W.; Sanner, M. F.; Belew, R. K.; Goodsell, D. S.; Olson, A. J., AutoDock4 and AutoDockTools4: Automated docking with selective receptor flexibility. *J. Comput. Chem.* **2009,** *30* (16), 2785-2791.

13. Pettersen, E. F.; Goddard, T. D.; Huang, C. C.; Couch, G. S.; Greenblatt, D. M.; Meng, E. C.; Ferrin, T. E., UCSF Chimera—A visualization system for exploratory research and analysis. *J. Comput. Chem.* **2004,** *25* (13), 1605-1612.

14. McDonald, I. K.; Thornton, J. M., Satisfying Hydrogen Bonding Potential in Proteins. *J. Mol. Biol.* **1994,** *238* (5), 777-793.